

MANIPULATOR BASE PLACEMENT SOLVED WITH HEURISTIC SEARCH

Edwin Francis Cárdenas Correa, edwin@ufrj.br¹
Max Suell Dutra, max@mecanica.coppe.ufrj.br²

¹COPPE/UF RJ, Programa de Engenharia Mecânica, Universidade Federal do Rio de Janeiro, Cidade Universitária, Centro de Tecnologia, Laboratório de Robótica, Bloco I-101, Rio de Janeiro, RJ, Brasil.

²COPPE/UF RJ, Programa de Engenharia Mecânica, Universidade Federal do Rio de Janeiro, Cidade Universitária, Centro de Tecnologia, Bloco G, Sala 204, Rio de Janeiro, RJ, Brasil.

Abstract. *In some cases, the decision to place the robot base is based on human judgments like symmetry and space available into manufacturing cells, yet this not guaranteed the best position of robot respect to some parameter, such as dexterity or energy consumption. This paper proposes a method to locate the frame base of serial manipulators using energy calculation and heuristic search, specifically describes the behavior of a six-degree-of-freedom industrial robot based on dynamic simulations for point-to-point operations. The results are restricted to classic joint trajectory planning and the success of the proposed methodology is compared with the base placement using symmetry.*

Keywords *Ant colony system, placement optimization, robot manipulator, heuristic search.*

1. INTRODUCTION

The robotics systems that include hardware and software control demands an amount of energy for operating, when movements are fast and repetitive the power consumption will become an important issue. For robots manipulators, there are two types of trajectories: point-to-point motion and motion through a predefined curve for end-effector. The first type is used for pick-and-place operations; the second is used in continuing operations of end-effector like cutting and welding. Trajectory planning handles the end-effector coordinates using the position, velocity and acceleration profiles of joints when the start and end points of the trajectory are predefined and fixed in the workspace. A review of trajectory planning techniques is shown in (Spong et al., 2006) and (Siciliano, 2009).

Determining the optimum location of base for a predefined path to be followed by the end-effector in his workspace requires one or more criteria. In last two decades diverse studies have dealt with the manipulator base placement but there is not a predominant theory. Below is presented a brief description of the work of various researchers.

Some studies addressed optimal placement of a robotic manipulator using the manipulability measure as the optimization criterion (Aspragathos & Foussias, 2002; Nelson & Donath, 1990) but these criteria cannot describe the aptitude of a manipulator to move in a given direction. (Fardanesh & Rastegar, 1988) propose velocity and cycle time criterion and (Feddema, 1996) find the optimal position of the robot base given a fixed set of points in a workspace which the robot end-effector must reach.

Others optimization strategies studied by (Pamanes-García et al., 2008; Pamanes & Zeghloul, 1991) includes multiple kinematic indices, joint-limits and obstacle avoidance. The optimal placement using actuator torque requirements was studied by (Chou & Sadler, 1993), and (Hsu et al., 1999) studied the problem of where to place the base manipulator in a factory environment for collision-free tasks.

(Abdel-Malek et al., 2004) propose a numerical method for the placement of robot manipulators based on maximizing the dexterity at specified target points. (Santos, 2010) take both kinematics and dynamic features into placement strategy. An approach to optimize the location of a given path within the workspace of a manipulator in order to minimize the electric energy consumed by its actuators is introduced by (Ur-Rehman et al., 2009).

In this paper directly addresses the concept of estimated energy to move the end-effector from point P_A to P_B (see Fig. 1) using dynamic calculations for a singular placement of the robot. With identical start and goal end-effector coordinates, a heuristic strategy finds the nearest-best robot position with the lowest power consumption. For the same pick-and-place operation, different robot positions produce different curves of end-effector through in his workspace, this condition is valid for restricted and isolated areas, such as robotic manufacturing cells. The complete formulation using collision-free path planning is a subject for future research.

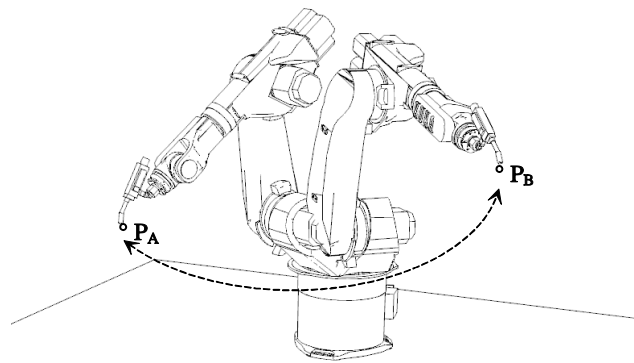


Figure 1. Start and goal configurations for point-to-point motion of 6-DOF Arm. P_A and P_B are the initial and final coordinates of the end-effector. 3D models were taken from <http://www.kuka-robotics.com>

This paper is organized as follows. Section 2 contains the description of 6 degrees of freedom normalized serial robot used to get the analytical expressions and simulations performed. Section 3 derives the estimated energy and the concept of distribution criterion for minimizing energy required. Section 4 explains the heuristic search algorithms based on Ant Colony System to find the best position of the manipulator. Section 5 presents the tests and results obtained from simulations using MATLAB known as a numerical computing environment engineering and programming language widely used. Finally, in Section 6 shows some conclusions and discuss ideas for future work.

2. ROBOT FRAMEWORK

2.1. Kinematics Description

The anthropomorphic robots with 6 degrees of freedom (6-DOF Arm) are widely used in industry; these robots generally have the last three degrees of freedom coincident in the same point in space called "wrist". The calculation of the coordinates of the end-effector as a function of joint coordinates is known as forward kinematics. The description kinematics of 6-DOF Arm is given by the Tab. 1 with the Denavith-Hartenberg parameter matrix, using modified notation according to classic theory (Craig, 2005; Jazar, 2010).

Table 1. Denavith-Hartenberg parameters for 6 DoF Arm Manipulator.

i	a_{i-1}	α_{i-1}	d_{i-1}	θ_i
1	0	0	a_1	θ_1
2	0	$\pi/2$	0	θ_2
3	a_2	0	0	θ_3
4	0	$\pi/2$	a_3	θ_4
5	0	$-\pi/2$	0	θ_5
6	0	$\pi/2$	0	θ_6

Normalized values: $a_1 = a_2 = a_3 = 1$ m.

2.2. Joint Space Trajectories

The process to obtain a robot configuration (joint angles) based on desired end effector coordinates is called inverse kinematics, one or more solutions can be achieved. This paper uses the exact values of the inverse kinematics provided by the trigonometric approach in (Tsai, 1999).

In point-to-point motion, the manipulator requires making a motion from an initial to a final configuration in a given time t_f . In this case, the actual end-effector path is of no concern. It is obvious that infinite solutions exist for this problem, assumed that the rotation is executed through a torque τ supplied by a motor, a solution can be found which minimizes the energy dissipated in the motor. The choice of a third-order polynomial function to generate a joint trajectory represents a valid solution for the problem at issue (Siciliano, 2009). So, joint motion is determinate by:

$$\theta(t) = c_3 t^3 + c_2 t^2 + c_1 t + c_0 \quad (1)$$

Then the velocity and acceleration profiles are:

$$\dot{\theta}(t) = 3c_3 t^2 + 2c_2 t + c_1 \quad (2)$$

$$\ddot{\theta}(t) = 6c_3t + 2c_2 \quad (3)$$

The four polynomial coefficients, c_i can be found by solving the Eq. (4), using the initial θ_{start} and final θ_{goal} configurations (for each joint) and assuming value for the initial and final joint velocities, which are usually zero.

$$\begin{aligned} c_0 &= \theta_{start} \\ c_1 &= \dot{\theta}_{start} \\ c_3t_f^3 + c_2t_f + c_1t_f + c_0 &= \theta_{goal} \\ 3c_3t_f^2 + c_2t_f + c_1 &= \dot{\theta}_{goal} \end{aligned} \quad (4)$$

3. ESTIMATING ENERGY AND MINIMIZED CRITERION

The aim of this paper is to show how to find a good position of the base of the manipulator using an estimated of power consumption when the robot moves from point P_A to P_B . Although a realistic calculation is provided by electrical models in actuators in each joint i , a generalization of estimated energy is given by the dynamics using calculating the joint torques necessary for the execution of the trajectory. In this case an efficient joint torque calculation is provided using the recursive Newton-Euler formulation (Siciliano & Khatib, 2008), which consists to find in order the vectors torque τ_i corresponding to set vectors $\theta_i, \dot{\theta}_i, \ddot{\theta}_i$ governed by joint space trajectories.

Assuming in our case the largest energy contribution is given by the first three degrees of freedom, the dynamics calculations were performed using the mass values of the first three links as $m_1, m_2, m_3 = 10$ kg. And each center of mass is located at the midpoint of the link like a thin rectangular bar.

The Newton-Euler formulation method gives us a set of equations by torque analysis in function of time. Then is possible find the estimated energy by the first three degrees of freedom using Eq. (5):

$$E_t = \sum_{i=1}^3 \left(\int_0^{t_f} \tau_i(t) \omega_i(t) dt \right) \quad (5)$$

Where τ_i is torque in joint i , and ω_i is angular velocity associated. ω_i is directly calculated with a Newton-Euler formulation of the robot (or N-E dynamic to simplify).

The first idea to calculate the location of the robot is to minimize the Eq. (5) for a set of vectors $[O_x, O_y, O_z]^T$ corresponding to the possible base coordinates of the manipulator. Here is introduced a second criteria, the concept of *index energy-distribution* (index-ed). The distributed energy is a controversial definition, because the energy always is a scalar and computing the energy equilibrium between the joints is an interesting issue. For example, for a single joint could have increased energy while the other joints only work at low loads, this condition could result in premature maintenance procedures.

Figure 2 shows the distribution (index-ed) like a magnitude of the resulting vector when using scalar energy quantities as orthogonal components. This concept is not limited to a three-dimensional framework and can be easily extrapolated n -dimensional space, such as multi-robots systems and high redundant robots. Another conception of index-ed could be the sum of energies with weights by joint, but this idea is for future studies.

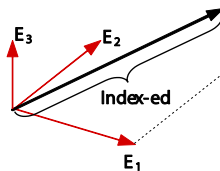


Figure 2. Index energy-distribution concept. E_1, E_2 and E_3 are the energy contribution by joint.

The index-ed depends of three energy contributions, the difference with the index provide by Eq. (5) is that, the index-ed has several values for the same value $E_t = |E_1| + |E_2| + |E_3|$. The lowest index-ed is achieved when the individual magnitudes $|E_i|$ tend to be the same.

4. HEURISTIC SEARCH

For a particular position $O = [O_x, O_y, O_z]^T$ of the base of robot, is possible to calculate the index-ed for a specific trajectory. Therefore, finding the best values $O_x, O_y,$ and $O_z,$ that generate a lower index, can be considered as a combinatorial problem for discrete set of data of $x, y,$ and z for base coordinates.

One way to find the relationship between discrete data x , y , and z , is using the ant colony heuristic strategy proposed by (Marco Dorigo & Stützle, 2004). The Ant Colony System algorithm or ACS, is an effective algorithm to solve combinatorial problems such as TSPs or Travelling Salesman Problems (M. Dorigo & Gambardella, 1997). The Fig. 3 shows a variation of the ACS original, this variation is denominated PACS (Position-ACS) because that is able to solve the base placement problem.

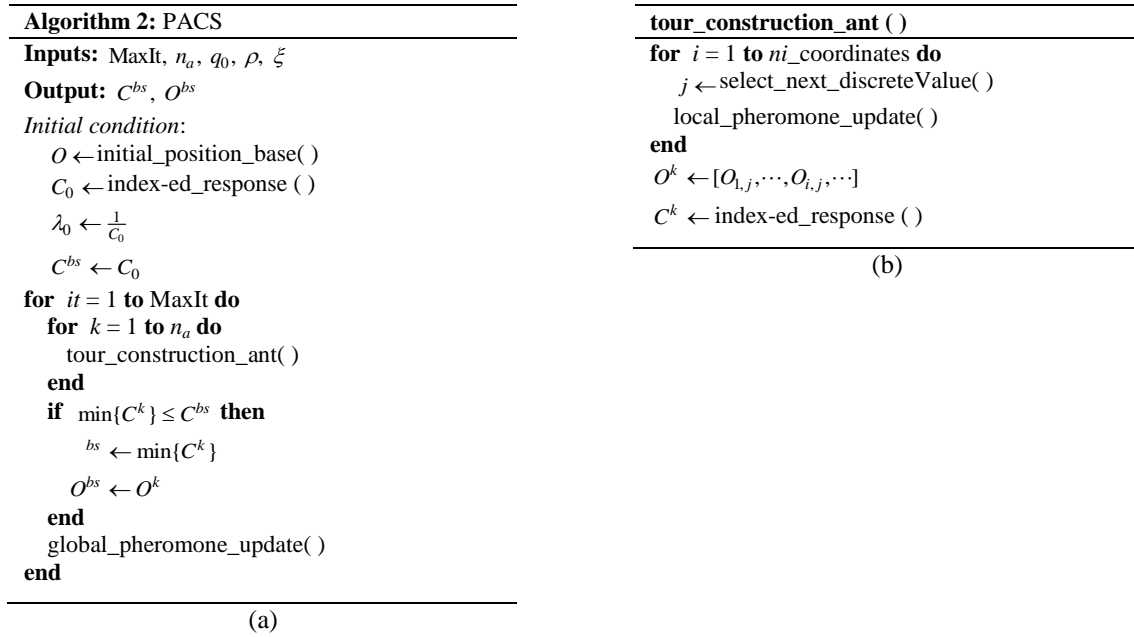


Figure 3. (a) Algorithm for positioning the base of the robot, using Ant Colony System approach. (b) tour_construction_ant function.

The heuristic PACS algorithm requires an initial position O of the frame base robot. The result of the *initial_position_base* function is usually the human concept of positioning of the base. C_0 is the value of index-ed of initial position O , provided by the N-E dynamic of robot.

The λ_0 is the initial level of pheromone for all discrete values of O . C^{bs} and O^{bs} are the best-so-far solutions found by the algorithm, C^{bs} and O^{bs} correspond to index-ed and vector of coordinates of base robot.

The stop criterion is the maximum number of iterations MaxIt. A single ant k provides a single solution C^k , for n_a ant set the best solution ($\min\{C^k\}$) by iteration it is compared with C^{bs} to actualize the global solution C^{bs} and O^{bs} .

In our study case, the set of discrete values $O_{i,j}$ corresponds to three sets: $O_{x,j} = [O_{x,1}, \dots, O_{x,nx}]$, $O_{y,j} = [O_{y,1}, \dots, O_{y,ny}]$ and $O_{z,j} = [O_{z,1}, \dots, O_{z,nz}]$ which are all possible coordinates of robot base. Each $O_{i,j}$ has a $\lambda_{i,j}$ level of pheromone. In each iteration it , the best solution O^{bs} has a *global_pheromone_update* with the expression:

$$\lambda_{i,j} = (1 - \rho)\lambda_{i,j} + \rho \Delta \lambda_{i,j}^{bs}, \quad \forall (i, j) \in O_{i,j} \quad (6)$$

Where the increasing pheromone for the best-so-far solution is $\Delta \lambda_{i,j}^{bs} = C^{bs}$.

In PACS, an ant selects a vector coordinates O^k using *tour_construction_ant* function (Fig. 3b). In the study case the $ni_coordinates = 3$, corresponding to a three-dimensional search space. A discrete value j is chosen according to the so called pseudorandom proportional rule, given by

$$j = \begin{cases} \arg \max\{\lambda_{i,j}\}, & \text{if } q \leq q_0 \\ J, & \text{otherwise} \end{cases} \quad (7)$$

Where q is a random variable uniformly distributed in $[0,1]$, q_0 ($0 \leq q_0 \leq 1$) is a parameter, and J is a random variable selected according to the probability distribution given by Eq. (8), with $\alpha = 1$. Tuning the parameter q_0 allows modulation of the degree of exploration and the choice of whether to concentrate the search on the system around the best-so-far solution or to explore other tours (Marco Dorigo & Stützle, 2004).

$$p_{i,j}^k = \frac{(\lambda_{i,j})^\alpha}{\sum (\lambda_{i,j})^\alpha} \quad (8)$$

The difference between ACS and PACS lies that the ACS algorithm has a parameter adjustment η due to the distance between cities for TSP problems, while PACS contemplates that parameter indirect with index-ed.

In addition to the *global_pheromone_update*, in PACS the ants use a *local_pheromone_update* that they apply immediately after having chose j value during the tour construction:

$$\lambda_{i,j} = (1 - \xi) \lambda_{i,j} + \xi \lambda_0 \quad (9)$$

Where, $0 < \xi < 1$, in majority of cases $\xi = 0.1$ (Marco Dorigo & Stützle, 2004).

Usually for serial manipulators a particular joint torque is higher than the others. For example, in the case of 6-DOF Arm, the τ_2 is always larger than others (as discussed in the following sections), therefore, the major contribution to the energy expended by the manipulator is due to the second joint. In that vein, a version of the PACS algorithm that adopts the critic-torque of robotic system directly into the heuristic search is the PACS-T (PACS with Torque influence).

PACS-T has the same PACS algorithmic structure (Fig. 4). The difference lies in two aspects: first, the function *index-ed_response* is exchanged for *total-energy_response* of the system, provided by Eq. (5). And second, the new parameter γ that modulates the influence of value of critic-torque in the heuristic search. The critic-torque τ_{critic} is function of time, indeed it is easy estimated by robot dynamics. For example, in the 6-DOF arm $\tau_2 = \tau_{critic}$ and his function in the time is determined by Newton-Euler formulation method. The highest value of critic-torque is obtained with $\max\{\tau_{critic}(t)\}$. In addition, the γ value can be adjusted agree with real torque restrictions of the actuator.

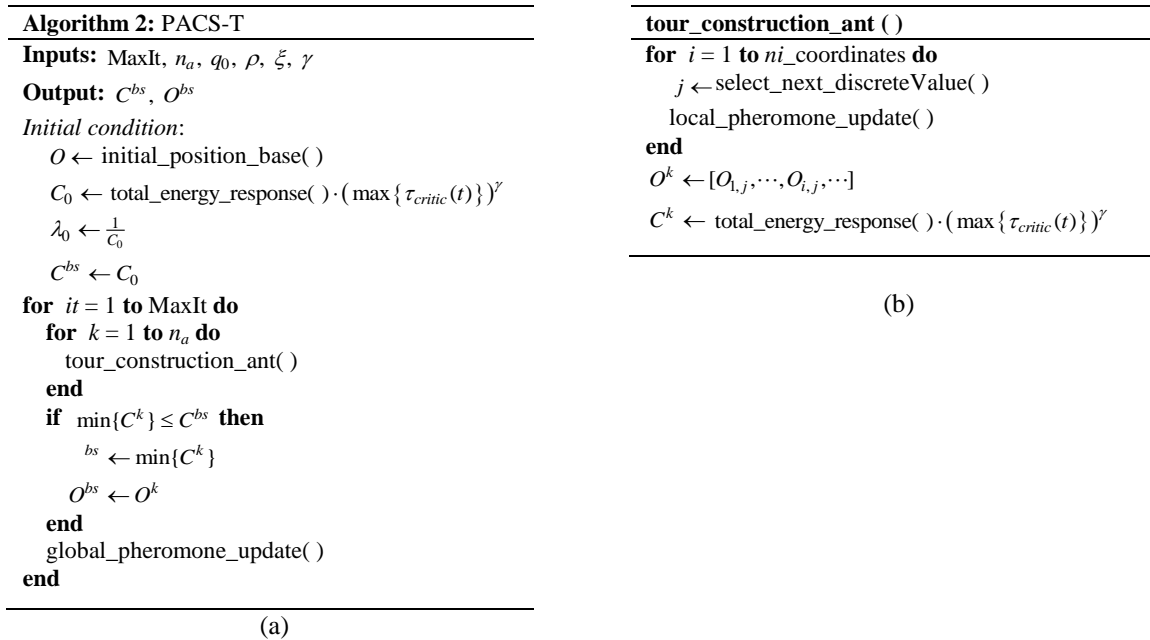


Figure 4. (a) Version of PACS algorithm with influence of critic-torque. (b) *tour_construction_ant* function.

5. SIMULATIONS AND RESULTS

This section displays the tests performed in the MATLAB environment, as well as qualitative analysis of the behavior of algorithms proposed. Five examples are showed into three subsections. All examples use a same normalized 6-DOF Arm robot already explained, meanwhile all initial base position were designated by the concept of symmetry and human judgment

5.1. Three-dimensional Search Space Condition

In the following example, a search space is generated as a volume where the manipulator can operate. Figure 5 shows the initial conditions where the search space is a cube (Fig. 6). The objective is to obtain the better position of robot for initial and final coordinates P_A and P_B of end-effector, his path is governed by joint space trajectories and the gray obstacle is only illustrative for a typical pick-and-place operation.

The vector sets that limit the search space for examples 1 and 2 are:

Example 1: $x = [-1 : 0.01 : 0]$, $y = [-1 : 0.01 : 0]$, $z = [-0.5 : 0.01 : 0.5]$. 201 discrete values for each coordinate.

Example 2: $x = [-1 : 0.01 : 0]$, $y = [-1 : 0.01 : 0]$, $z = [0 : 0.01 : 1]$. 201 discrete values for each coordinate.

In Fig. 6 depicts the results applying PACS for examples 1 and 2. All the examples the parameters were adjusted as follows: $MaxIt = 100$; $n_a = 5$; $q_0 = 0.7$; $\rho = 0.08$ and $\chi = 0.1$.

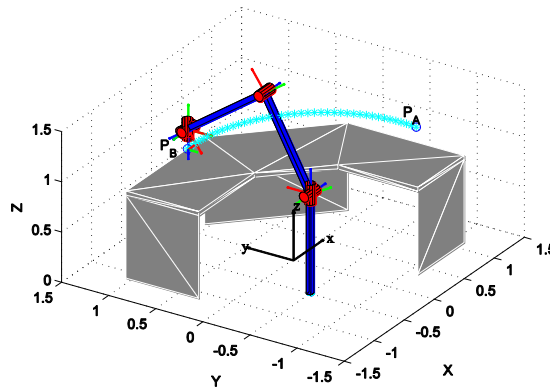


Figure 5. Representation of the initial base condition for the examples 1 and 2. The base robot coordinates were tuned by symmetry with the end-effector coordinates and the hypothetical limit of available floor.

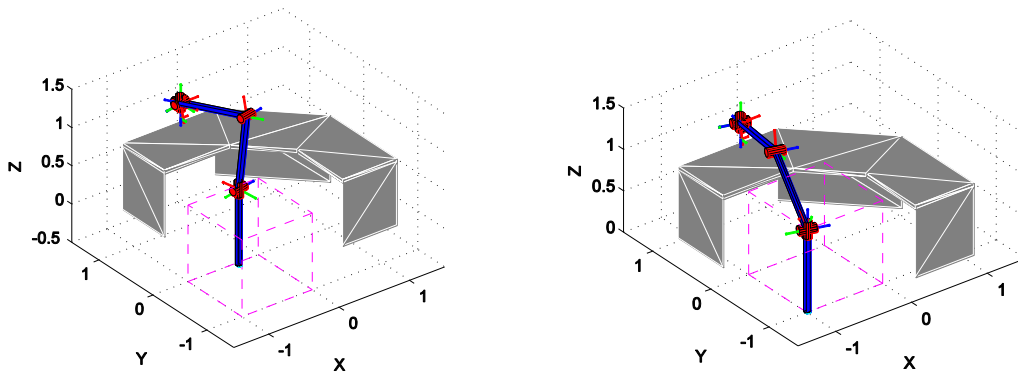


Figure 6. (a) and (b) are the graphical results applying PACS algorithm to examples 1 and 2 respectively. The dashed line represents the search space.

The results yielded by these examples provides always solutions in bottom of the search space in z coordinate. This can be explained because some singular configurations provide the lower value of reaction force at each joint, as can be explained by stiffness analysis of serial manipulators (Tsai, 1999). In this case the arm with an extended configuration and perpendicular to the floor makes the forces to propagate from the end-effector toward the floor using the structure of the robot. The joint actuators suffer less torque and therefore there is less total energy expenditure. Indeed the singular configurations result in loss of manipulability (Siciliano, 2009), but if the robot is capable of performing the proposed trajectory this condition is not necessarily bad.

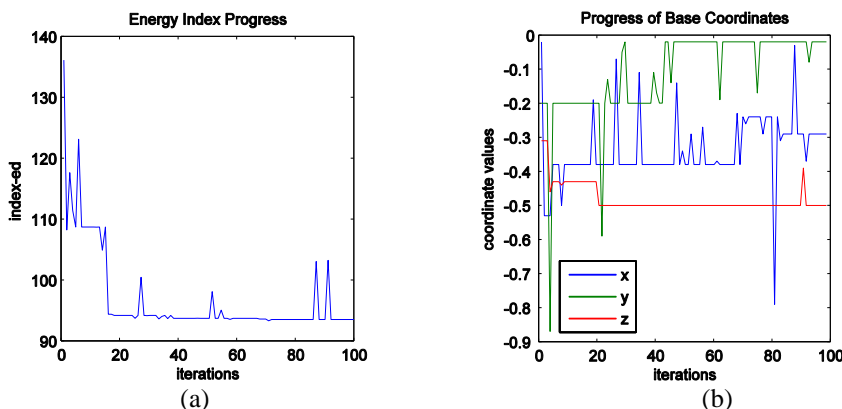


Figure 7. Typical results of heuristic search of PACS algorithm. (a) Progression of energy optimization process using ACS. (b) Base coordinates tendency using PACS in the example 1.

The Fig. 7a is the energy index progress of a typical heuristic search using PACS algorithm. Fig. 7b shows how change the base coordinate values through the iterations of heuristic search for example 1.

5.2. Two-dimensional Search Space Condition

Example 3: In this case, end-effector requires to move from $P_A = [1.2 \ 0.8 \ 0.6]^T$ to $P_B = [1.4 \ -0.6 \ 1.2]^T$, the search space is a rectangular area in X-Y plane defined by the discrete values: $x = [-1:0.01:1]$, and $y = [-1:0.01:1]$. The initial position of the base is: $O = [0 \ 0 \ 0]^T$.

The 200 discrete values, for each coordinate, produces $4E+4$ possible solutions. A surface representation of the index-ed behavior for the example 3 is shown in Fig.8a. This surface has a zero value region at left side, this occurs due to the kinematic inability of robot to reach the point P_A or P_B by the end-effector. PACS obtains solutions in general very close to optimal value, however, exist an interesting sub-optimal solution. The two solution exhibits similar index-ed, but the sub-optimal solution provides robot configurations near to singularity situation when the joint 3 (elbow) tend to 180° (Fig. 8b and 8c.)

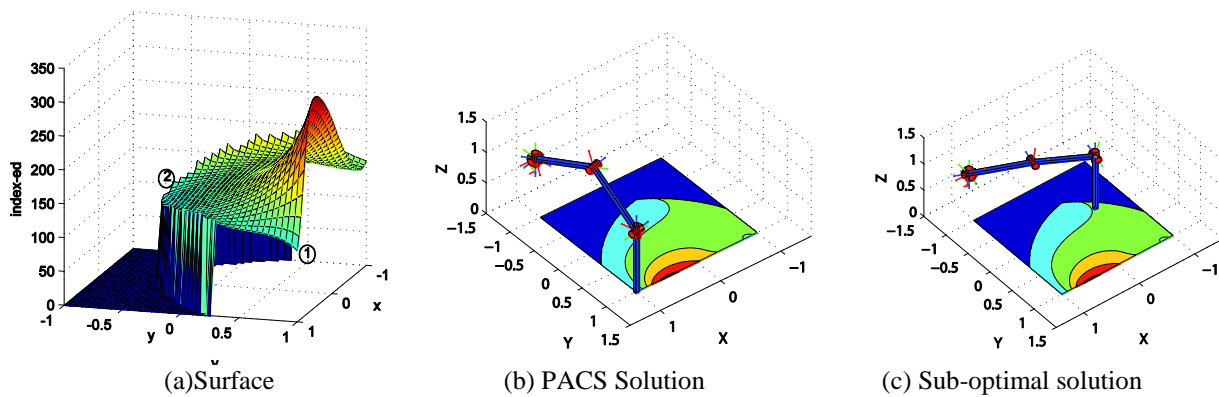


Figure 8. Index-ed surface generated with the restrictions of example 3. (1) PACS solution: $O = [1 \ 1 \ 0]^T$, Index-ed = 105.35. (2) Sub-optimal solution: $O = [-0.5 \ -0.13 \ 0]^T$, Index-ed = 112.57

Moreover, the torques obtained in the second link to the sub-optimal solution have higher values than the values obtained with the algorithm PACS, as is shown in Fig. 9. In addition, the PACS solution has the torque curves with better distribution of loads, therefore the index fulfills its function to distribute the energy consumption under the torque required between the joints. This assumption is valid from the point of view of design, for a real robot with specifications the torque supply, the methodology must be reformulated as in PACS-T algorithm.

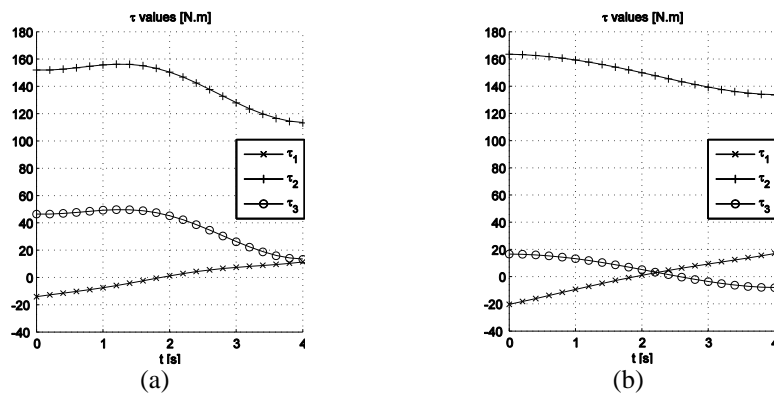


Figure 9. Torque profiles for Example 3: (a) PACS solution. (b) Sub-optimal solution.

Example 4: This is an ideal case, where P_A and P_B points are in the search area which is large enough to observe the behavior of the index-ed of the robot for all possible positions. The parameters are:

$$P_A = [0.8 \ 0 \ 1]^T, P_B = [-0.8 \ 0 \ 1.15]^T, -2 > x > 2, \text{ and } -2 > y > 2.$$

Figure. 10a illustrates the behavior complete of the index-ed in a particular case of point-to-point operation of example 4 and the Fig. 10b shows his contour plot. Certainly this example shows that with different size of the search space the solution obtained is different. A good selection of search space improves performance of the search algorithm avoiding the areas where there is no response.

Moreover, the intuitive idea of placing the robot in the middle of the two operating points PA and PB, increases robot energy consumption (central peaks in Fig. 10a). This can be explained by the fact that the joints must execute large movements in a short time, making large angular velocities, therefore energy spending is higher.

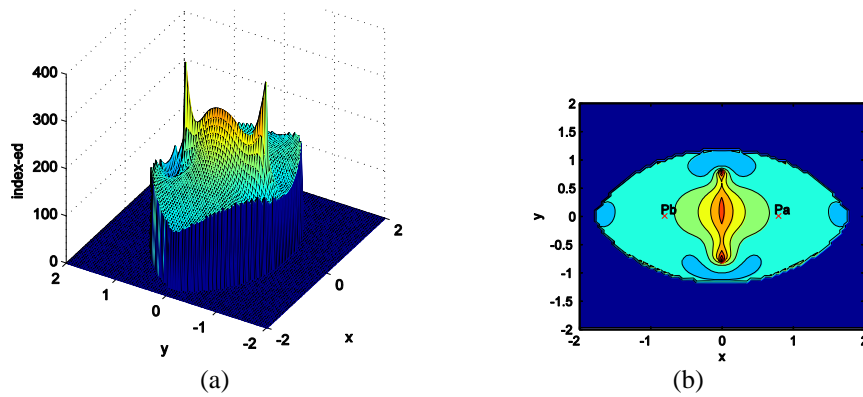


Figure 10. A total index-ed behavior, particular case of example 4 with an area large enough search space.

5.2. Two-dimensional Search Space Condition

The previous section showed how to locate the base robot using the index-ed criterion. The heuristic search of the PACS can also use other criteria as the total energy estimated by Eq. (5). When the main restriction for manipulator performance is the critic-torque, the PACS-T algorithm can be used to solve the system. This section presents a comparison between PACS and PACS-T algorithms.

Similarity of example 4, the Fig. 11a shows the contour plot of surface generating for the example 3 using PACS, the Fig. 11b is the contour plot of estimating energy using Eq. (5) by same example, this condition is exactly the definition of PACS-T with $\gamma = 0$ (maximum torque value is not considered).

The Fig. 11a and Fig. 11b are very similar; the surfaces have the same shape, nevertheless, in this case the exclusive use of the estimated energy in Fig. 11b causes strong local minimal solutions near to singular configurations resulting in high torques in the joints, like sub-optimal solution of Fig. 8c.

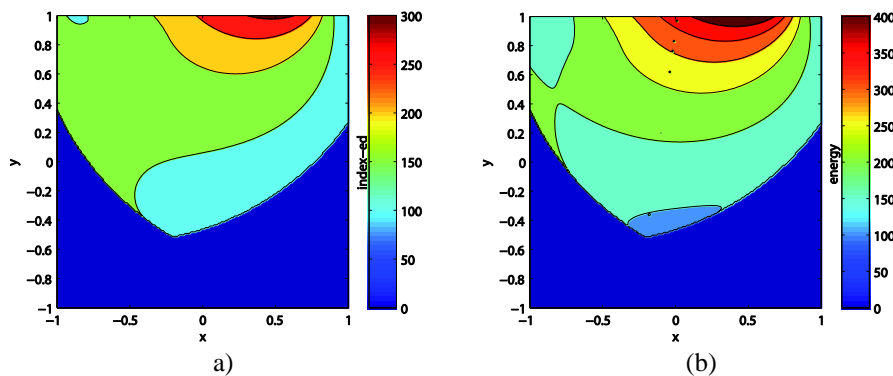


Figure 11. Contour plots for Example 3 using: (a) Index-ed. (b) Energy level.

Table 2 shows a comparison summary of the performance of heuristic algorithms for solving the example 3. Using PACS-T and $\gamma = 0$, the solution has lower energy consumed, but increases the maximum critic-torque value (joint 2). When the value of γ is increased, the solutions provided by PACS-T become closer to the values given by PACS, as well as the maximum value of a critic-torque decreases.

Table 2. Comparison of strategies applied to example 3.

Strategy	O_B [m]	Index-ed	Energy [J]	$\max(\tau_{critic})$
Human	[0 0 0]	146.1936	184.3217	161.622
PACS	[1 1 0]	105.3493	151.7841	156.2789
PACS-T, $\gamma=0$	[-0.48 -0.05 0]	113.4210	127.2846	165.4815
PACS-T, $\gamma=1$	[-0.46 -0.01 0]	115.3836	130.6709	166.2080
PACS-T, $\gamma=2$	[-0.49 -0.25 0]	129.3983	136.9266	154.9250
PACS-T, $\gamma=4$	[0.58 0.95 0]	134.5428	184.5890	144.6354

For the example 3, PACS achieved a better balance between energy expended and the maximum value of the critical-torque. PACS and PACS-T use heuristic search which is based on discrete ant colony system, for this reason the comparative results of the Table 2 between Index-ed and energy requirement with torque-influence are an approximation, and this results show only a tendency obtain with the methodology proposed here. Finally, both strategies PACS and PACS-T obtain in all instances better results than the location based on symmetry and human decision.

Additionally, the example 5 illustrates a typical application where is requires a quick pick-and-place operation. The initial and final position of end-effector are symmetrical to the robot, so that the base is located in the best way respect to a symmetry and human judgment. Obviously, many restrictions can be changed to test the algorithms and these types of heuristic strategies have weak mathematical proofs therefore an intention of this paper is to show the key issues to apply the heuristic search to base placement problem, like the following example:

Example 5: The values of initial and final position of the end effector are close one from the other, $P_A = [0.5 \ -1 \ 1]^T$ to $P_B = [-0.5 \ 1 \ 1]^T$. The search space is defined by the discrete values: $x = [-1:0.01:1]$, and $y = [-1:0.01:1]$. And the initial position of the base is given by the coordinates $O = [0.5 \ 0.5 \ 0]^T$.

Table 3 shows the results of example 5 and the solutions are represented in Fig. 12. The results are very similar to those obtained in previous cases and this confirms that search heuristic provides better results than the initial position of base-robot adjusted by human criterion. Moreover, the performance of PACS and PACS-T are substantially equal in this case.

Table 3. Comparison of strategies applied to example 5.

Strategy	O_B [m]	Index-ed	Energy [J]	$\max(\tau_{critic})$
Human	[-0.5 -0.5 0]	262.1914	352.1924	131.4952
PACS	[-1 -0.78 0]	211.7246	259.0141	146.3006
PACS-T, $\gamma=1$	[-1 -0.72 0]	212.2576	262.1373	144.4369

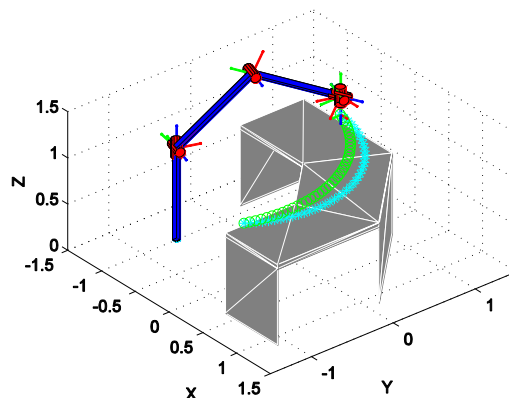


Figure 12. Trajectory plots of solutions for Example 5. Initial position in cyan asterisks (human concept). The PACS solution draws in green circles.

6. CONCLUSIONS

This work shown how to obtain the position of base frame coordinates of a serial manipulator through the heuristic search. The ant colony system was used as iterative heuristic search, the proposed algorithm works fine with energy minimization criteria based on Newton-Euler dynamics calculation and closed-form solution of inverse kinematics.

Two algorithms were developed, the first is based on the concept of energy distribution and the second is based on the influence of a critical-torque that affects the behavior of the robotic system. Both algorithms showed better performance than the use of human judgment based on the symmetry and the space available.

Although the proposed method was tested for pick-and-place operations, where end-effector path is of no concern, this methodology can be extrapolated for continuous operations for the end-effector as cutting and painting operations.

The results of the simulations suggest that in some cases the configurations near to kinematic singularities of manipulator provides less energy consumption; therefore in the future, it would be interesting to combine the concepts of estimated energy and dexterity.

Consequently, is recommending the use of these strategies based on energy consumption with restricted search areas, so that the singular configurations do not cause excessive torque on critical joints. Another interesting idea is to

apply the traditional control techniques or other mechanism that permits a more precise control over the adverse effects of the singular configurations.

The strategies shown here can be implemented in off-line robot programming software and to help the designers develop more efficient automated systems. A future work would consist to apply these strategies in multi-robot systems or in more complex tasks of robot manipulation.

7. REFERENCES

- Abdel-Malek, K., Yu, W. & Yang, J., 2004, "Placement of Robot Manipulators to Maximize Dexterity". *International Journal of Robotics and Automation*, 19, pp. 6-14.
- Aspragathos, N.A. & Foussias, S., 2002. "Optimal location of a robot path when considering velocity performance". *Robotica*, 20(2), pp. 139-147.
- Chou, H.C. & Sadler, J.P., 1993, "Optimal location of robot trajectories for minimization of actuator torque". *Mechanism and Machine Theory*, 28(1), pp. 145-158.
- Craig, J.J., 2005, "Introduction to robotics: mechanics and control". Upper Saddle River, N.J.: Pearson/Prentice Hall.
- Dorigo, M. & Gambardella, L.M., 1997, "Ant colony system: a cooperative learning approach to the traveling salesman problem". *Evolutionary Computation, IEEE Transactions on*, 1(1), pp. 53-66.
- Dorigo, M. & Stützle, T., 2004, "Ant colony optimization". Cambridge, Mass.: MIT Press.
- Fardanesh, B. & Rastegar, J., 1988), "Minimum cycle time location of a task in the workspace of a robot arm". In: *Decision and Control, 1988., Proceedings of the 27th IEEE Conference on*, vol.2283, pp. 2280-2283.
- Feddema, J.T., 1996, "Kinematically optimal robot placement for minimum time coordinated motion". In: *Robotics and Automation, 1996. Proceedings of 1996 IEEE International Conference, Vol. 4*, pp. 3395-3400.
- Hsu, D., Latcombe, J.C. & Sorkin, S., 1999, "Placing a robot manipulator amid obstacles for optimized execution". In: *Assembly and Task Planning, (ISATP '99) Proceedings of the 1999 IEEE International Symposium*, pp. 280-285.
- Jazar, R.N., 2010, "Theory of applied robotics : kinematics, dynamics, and control". New York; London: Springer.
- Nelson, B. & Donath, M., 1990, "Optimizing the location of assembly tasks in a manipulator's workspace". *Journal of Robotic Systems*, 7(6), pp. 791-811.
- Pamanes-García, J.A., Cuan-Durón, E. & Zeghloul, S., 2008, "Single and multi-objective optimization of path placement for redundant robotic manipulators". *Ingeniería, investigación y tecnología*, Vol. 9, pp. 231-257.
- Pamanes, G.J.A. & Zeghloul, S., 1991, "Optimal placement of robotic manipulators using multiple kinematic criteria". In: *Robotics and Automation, 1991. Proceedings of 1991 IEEE International Conference*, vol.931, pp. 933-938.
- Santos, R., 2010, "Optimal Task Placement of a Serial Robot Manipulator for Manipulability and Mechanical Power Optimization". *IIM Intelligent Information Management*, 02(09), pp. 512-525.
- Siciliano, B., 2009,. "Robotics modelling, planning and control". In. London: Springer.
- Siciliano, B. & Khatib, O. (2008). *Springer handbook of robotics*. Berlin: Springer.
- Spong, M.W., Hutchinson, S. & Vidyasagar, M., 2006, "Robot modeling and control". Hoboken, NJ: John Wiley & Sons.
- Tsai, L.-W., 1999, "Robot analysis: the mechanics of serial and parallel manipulators". New York: Wiley.
- Ur-Rehman, R., Caro, S., Chablat, D. & Wenger, P., 2009, "Path placement optimization of manipulators based on energy consumption: Application to the orthoglide 3-axis". *Trans Can Soc Mech Eng Transactions of the Canadian Society for Mechanical Engineering*, Vol. 33(3), pp. 523-541.

8. RESPONSIBILITY NOTICE

The authors are the only responsible for the printed material included in this paper.